# Implementing III–nitride light-emitting devices on silicon substrates

**Mike Cooke reports on recent advances in putting indium gallium nitride laser, superluminescent and light-emitting diodes on silicon using epitaxy and wafer-bonding technologies.**

Silicon has been the electronics material of choice since the 1960s when mass production of complementary metal-oxide-semiconductor (CMOS) integrated circuits opened the way to the multiple communication technologies that dominate our thought-world today, at least in the rich countries of the West and east Asia.

One of the main drivers of this trend has been the low cost of the basic material and its combination with silicon dioxide ($SiO_2$) insulation. These materials are also increasingly being deployed in photonics applications, but suffer from the lack of low-cost light generation in group IV semiconductors like silicon.

Combining light-emitting III–V semiconductors with silicon at low cost is the project of many research groups around the world. In the short-wavelength visible and ultraviolet ranges, that means 'group III' metal — gallium, indium and aluminium — nitrides.

Although silicon-substrate indium gallium nitride (InGaN) light-emitters should be manufacturable at less expense, efficiencies suffer from the energy-sapping effects of high defect levels. One problem has been that the lattice mismatch between silicon and gallium nitride (GaN) is about 17%. The thermal expansion mismatch is even greater — around 54%. The lattice/thermal mismatches are presently bridged by using various aluminium gallium nitride (AlGaN) alloy layers before the main device layers.

The integration of InGaN light generation into a silicon platform raises the prospect of complex visible-light photonics and optoelectronics through waveguides, photodetectors and CMOS drive and control circuitry.

Here we examine recent advances in putting InGaN laser, superluminescent and light-emitting diodes on silicon using epitaxy and wafer-bonding technologies.

## Reducing laser power losses

Researchers in China have reduced the point defects in InGaN laser diode (LD) material on silicon with the aim of reducing operating voltages and injection current and increasing device efficiency [Jianxun Liu et al, Optics Express, vol. 27, p25943, 2019]. Laser diodes on silicon tend to have high threshold currents and voltages, indicating high electrical and optical power losses.

The research team from Suzhou Institute of Nano-Tech and Nano-Bionics (SINANO), University of Science and Technology Beijing, and University of Science and Technology of China, developed a lower-temperature growth process and alternative material structure in particular layers to reduce threshold currents and voltages by an approximate factor of 2 (72mA/150mA, 4.7V/8.2V).

The laser diode material (Figure 1) was grown on (111) Si with metal-organic chemical vapor deposition (MOCVD). The n-GaN contact layer was 2.7μm, while the lower cladding was 1.2μm n-$Al_{0.05}Ga_{0.95}N$. The multiple quantum well (MQW) active layer consisted of three pairs of 2.7nm/12nm 770°C $In_{0.12}Ga_{0.88}N/In_{0.02}Ga_{0.98}N$. The top p-GaN contact was 30nm thick, and the electron layer (EBL) was $Al_{0.2}Ga_{0.8}N$.

Two laser diode material samples, A and B, were produced (Table 1). Sample B used cooler growth temperatures in the lower and upper waveguides (WGs), and in the p-type contact layer (CL) superlattices (SLs). Lower temperatures reduced thermal degradation of the MQW region and carbon incorporation from the organic precursors used.

Carbon tends to compensate, reducing the effectiveness of the magnesium doping used for the p-type layers needed for hole injection. This is expected to increase series resistance and operation voltage, adding to laser diode power losses. Lower carbon levels are also associated with lower optical absorption.

The researchers comment: "It is noted that the adoption of InGaN/GaN SL WG would cause little effect on the thermal conductivity of the laser diode structure, because there was only a trace amount (1% in average) of indium in such SL WGs (sample B), and the total

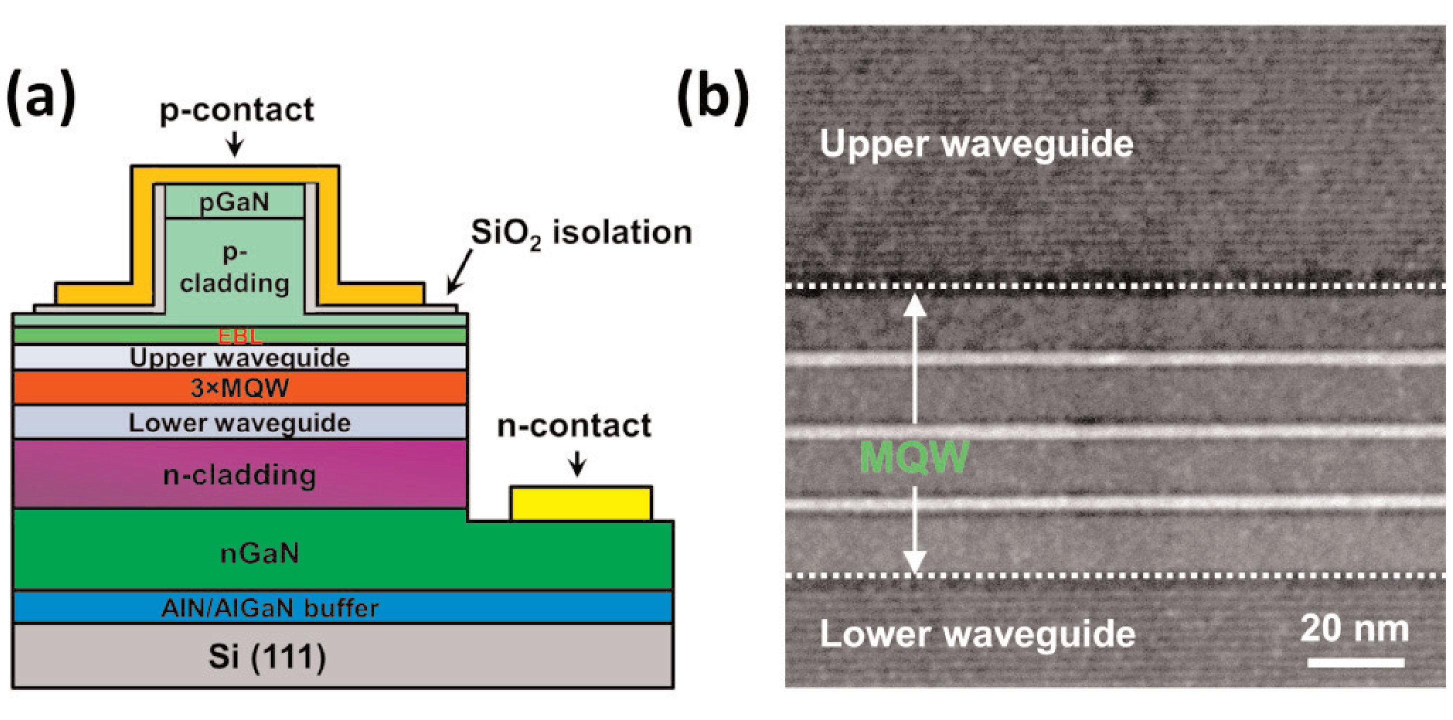

**Figure 1. (a) Schematic diagram of InGaN-based laser diodes grown on silicon. (b) Cross-sectional high-angle annular dark-field scanning transmission electron micrograph of InGaN MQW active region.**

thickness of the $In_{0.01}Ga_{0.99}N$ layer was only 70nm (40nm and 30nm for the lower and upper waveguide, respectively), which was negligibly smaller than that of the AlGaN cladding layers (1.8μm in total) and the n-GaN contact layers (2.7μm).”

Due to the lower growth temperatures, microscopic inspection of photoluminescence (PL) in sample B showed greater uniformity, compared with sample A. The more even PL suggests less degradation of the delicate MQW region. In addition, sample A suffered from a short decay time of 3.5ns, compared with 6.3ns for B, in time-resolved PL. The researchers suggest that the faster decay is due to non-radiative Shockley–Read–Hall (SRH) recombination through mid-gap defect levels. The team adds that SRH recombination results in reduced internal quantum efficiency (IQE, photons/electron) and increased junction temperatures and threshold currents.

The researchers also attribute some of the improvement in sample B’s IQE to replacement of the waveguide layer with InGaN SLs. The high-temperature GaN material tends to contain vacancies on the Ga ion site. Reducing the number of vacancies reduces optical absorption from strong band-tail effects. The silicon doping of the n-GaN layer also contributes band-tail energy states. “Such absorption will increase the internal optical loss and reduce the IQE, resulting in an increase in junction temperature and threshold current for the laser diodes,” the team writes.

The team fabricated edge-emitting laser diodes with ridges 800μm long and 4μm wide. The cleaved front and rear facets of the laser diodes were coated with titanium dioxide/silicon dioxide ($TiO_2/SiO_2$) multi-layers to increase reflectivity with low optical loss.

Electroluminescence experiments (Figure 2) demonstrated lasing peaks at 413.4nm and 418nm for samples A and B, respectively. The laser diodes were operated in 400ns pulse mode with 10kHz repetition to avoid self-heating effects. The wavelength difference is attributed tentatively to differences in MQW growth temperatures, which can significantly affect indium incorporation.

Sample B showed reduced threshold voltage — 4.7V, compared with 8.2V for sample A. The threshold current for B was also about half that of A: 72mA (2.25kA/cm$^2$) versus 150mA (4.7kA/cm$^2$). Reduced current and voltage, and hence input power, for a given output mean increased efficiency.

In lifetime tests under pulsed-mode operation, sample B laser diodes showed little degradation in output power after 620 hours, unlike devices based on sample A material.

►

**Table 1. Comparison of growth conditions between samples A and B.**

| Layer/Sample | A | B |
|---|---|---|
| p-type CL SL, 600nm | 950°C p-$Al_{0.11}Ga_{0.89}N$/GaN | 920°C p-$Al_{0.11}Ga_{0.89}N$/GaN |
| Upper WG, 60nm | 1050°C u-GaN | 770°C u-$In_{0.01}Ga_{0.99}N$/GaN SL |
| Lower WG, 80nm | 1050°C n-GaN | 770°C u-$In_{0.01}Ga_{0.99}N$//GaN SL |

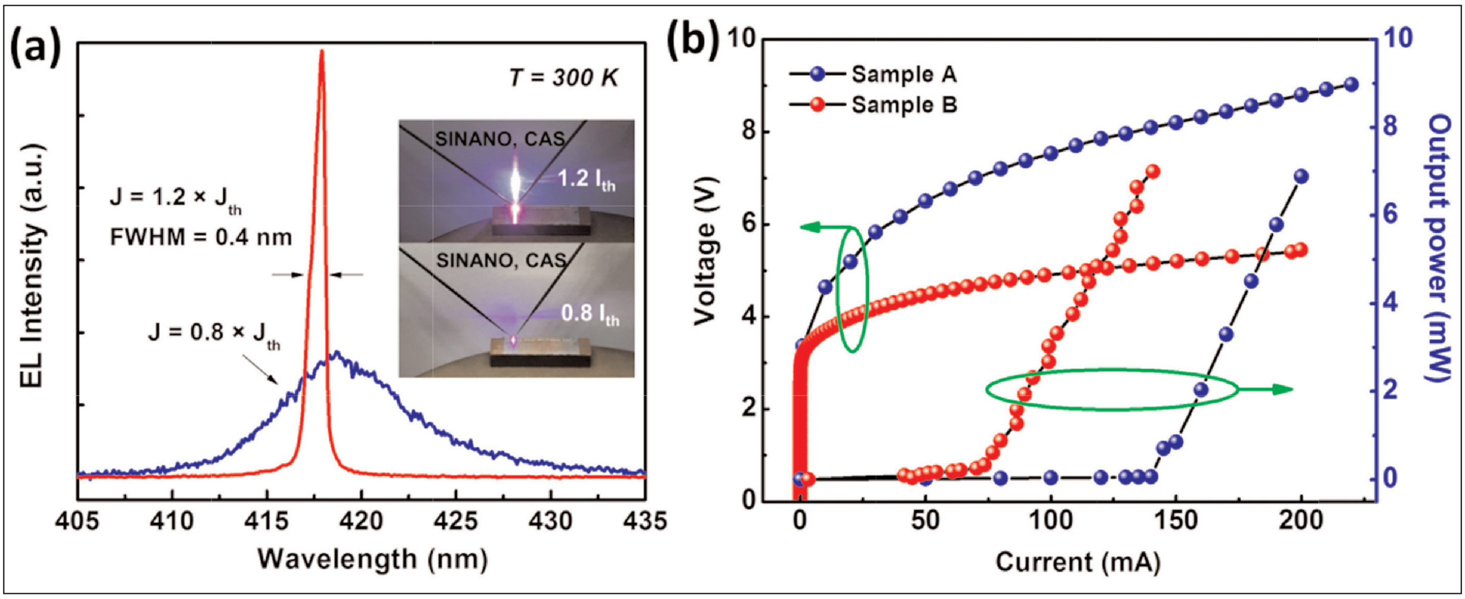

**Figure 2. (a) EL spectra of sample B above (1.2x) and below (0.8x) threshold current. Inset: corresponding far-field patterns. (b) On-bar light output power-current-voltage (L–I–V) characteristics under pulsed injection for samples A and B.**

## Superluminescent displays and communication

The same group of institutions, and many of the same researchers, have also developed InGaN superluminescent diodes (SLDs) monolithically integrated on silicon substrates [Jianxun Liu et al, ACS Photonics, vol6 (2019) no8, p2104]. The team sees opportunities for compact on-chip light sources for speckle-free displays and visible light communications (VLC).

The researchers used MOCVD on (111) Si substrates to create the III–nitride structure (Figure 3) for the SLD (Figure 4). The index-guided SLD featured a 4μm-wide ridge, which was J-shaped to suppress optical feedback oscillation in the 800μm-long cavity. Optical feedback runs the risk of laser action, which is not desired in SLDs. The J-bend of 6º occurred halfway down the cavity. The bend resulted in a facet that was not perpendicular to the cavity direction, allowing light to escape more easily.

The ridge waveguide and device mesa were formed with plasma etch. The p- and n-electrodes consisted, respectively, of palladium/platinum/gold and titanium/platinum/gold. After thinning, lapping and chemical mechanical planarization (CMP), the wafer was cleaved into bars containing 24 devices each. Comparison laser diodes were produced with straight waveguides. The devices were tested without packaging or facet coating.

The superluminescence of the device was demonstrated from the reduction in linewidth as the current injection increased from 400mA to 800mA, giving a reduction in full-width at half-maximum (FWHM) from 13.8nm (102meV) to 3.6nm (26meV), respectively (Figure 5). The main part of the reduction of FWHM occurred around 500mA when the value was 8.5nm (67meV), indicating the main onset of amplified spontaneous emission (ASE). In laser diodes, the reduction in FWHM is sharper, and generally results in linewidths narrower than 1nm — the fabricated comparison laser diodes had FWHMs of ~0.5nm (3.7meV) above threshold.

As the current through the SLD increased, there was at first a red-shift and then a blue-shift of the electrolumi-

| | | |
|---|---|---|
| Contact | $p^+$-GaN | 30nm |
| Cladding (p-type) | 132x($Al_{0.2}Ga_{0.8}N$/GaN) | 132x(1.5nm/3nm) |
| Electron blocking | p-$Al_{0.2}Ga_{0.8}N$ | 20nm |
| Waveguide | 30x($In_{0.02}Ga_{0.98}N$/GaN) | 30x(1nm/1nm) |
| Quantum wells | 3x($In_{0.12}Ga_{0.88}N/In_{0.02}Ga_{0.98}N$) | 3x(2.7nm/12nm) |
| Waveguide | 40x($In_{0.02}Ga_{0.98}N$/GaN) | 40x(1nm/1nm) |
| Cladding (n-type) | 14x($Al_{0.085}Ga_{0.915}N$/GaN) | 14x(75nm/10nm) |
| Contact | n-GaN | 1.3μm |
| Buffer | GaN | 1.4μm |
| Buffer | $Al_{0.17}Ga_{0.83}N$ | 450nm |
| Buffer | $Al_{0.35}Ga_{0.65}N$ | 340nm |
| Nucleation | AlN | 300nm |
| Substrate | (111) Si | |

**Figure 3. III–nitride epitaxial structure of SLD, using combinations of AlInGaN alloys.**

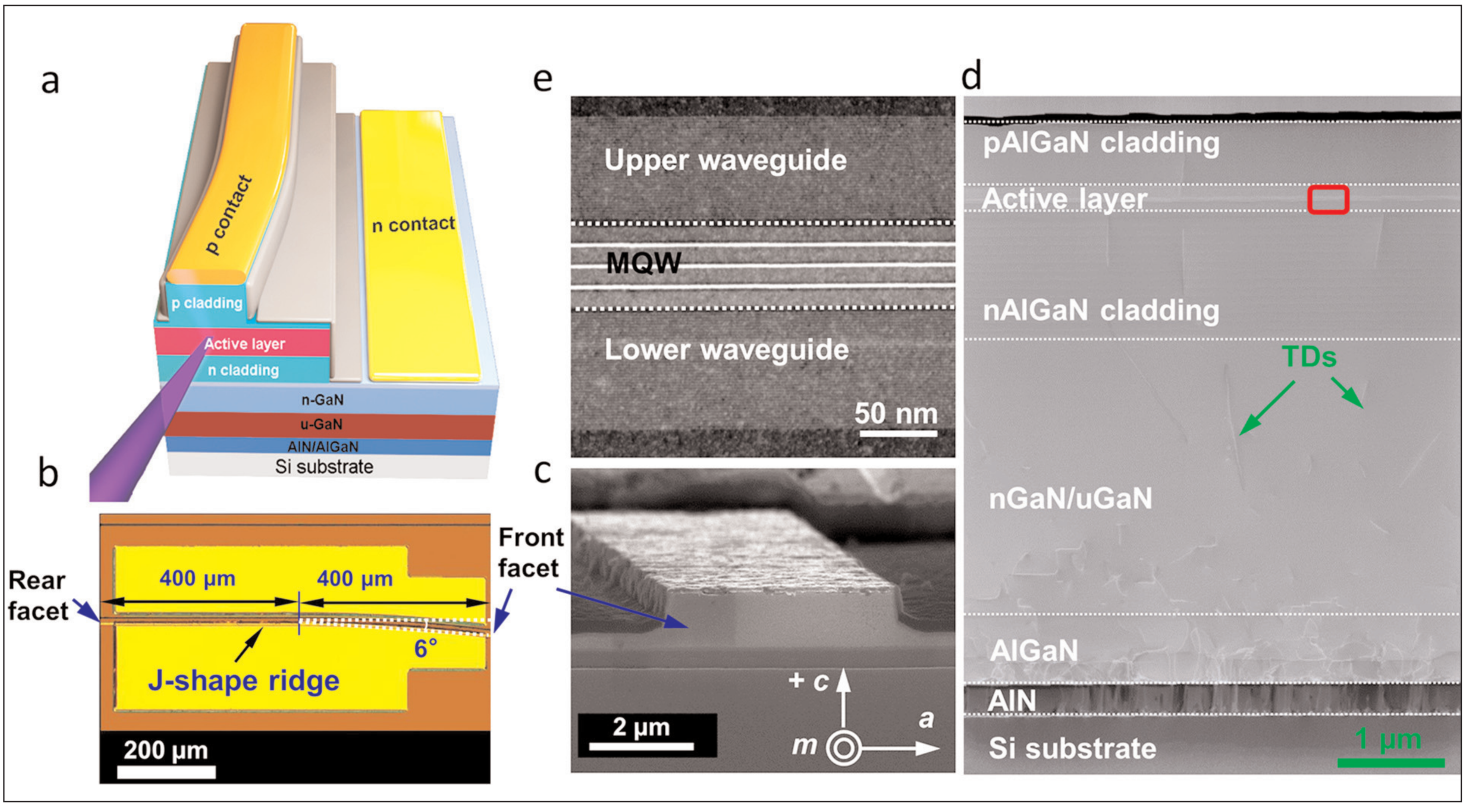

**Figure 4. (a) Three-dimensional illustration of InGaN-based SLDs grown on silicon with J-shaped ridge waveguide. (b) Top-view optical microscopy image of bar of InGaN-based SLDs after facet cleavage. (c) Scanning electron microscope image of cleavage facet. (d) Cross-sectional scanning transmission electron microscope (STEM) image. Total thickness of epitaxial layer was 5.8µm. (e) Enlarged STEM image of marked zone in (d).**

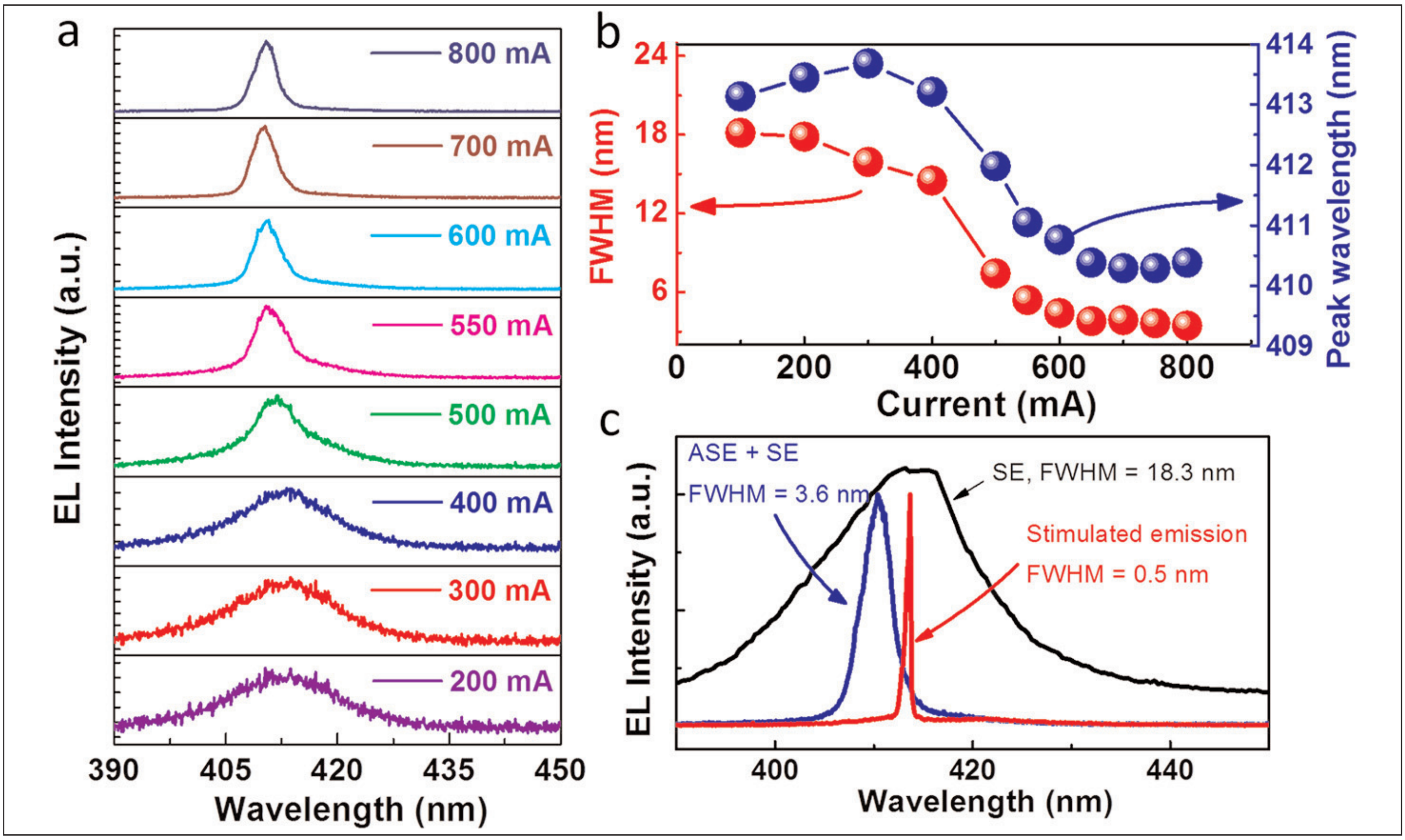

**Figure 5. (a) EL spectra of SLD under various pulsed injection current at room temperature. (b) Peak wavelength and FWHM as function of injection current. (c) Comparison of EL spectra for SLD below threshold (100mA), above threshold (800mA), and stimulated emission from laser diode (250mA) with identical epitaxial design.**

nescence (EL) peak wavelength. The researchers comment: "The observed red-shift under a low injection current can be attributed to the bandgap narrowing resulting from many-body effects. While the blue-shift of the EL peak under a high injection current can be explained by combined effects of the band-filling effect and the carrier-induced screening of the quantum-confined Stark effect." The quantum-confined Stark effect refers to the electric field that arises in III–nitride semiconductor heterostructures due to the charge-polarization of the chemical bonds. The effect tends to shift electron energy levels and to negatively impact electron-hole recombination into photons.

The transition from spontaneous emission to amplified spontaneous emission was also reflected in optical polarization measurements. Even below threshold, the emissions were dominated by the transverse electric (TE) modes of the waveguide structure. The degree of polarization, as expressed by the difference in TE and transverse magnetic (TM) emission relative to the total emission, increased from 84% to 97.6% between 400mA and 600mA injection. The 97.6% value is said to correspond to 20dB polarization extinction ratio (I make it 19dB, but I may have worked from a different definition).

Comparing SLD and comparison laser diode threshold currents, the former occurred around 550mA while the latter achieved lasing around 230mA, less than half the value of the SLD.

The SLD light output power began to saturate at 1100mA injection, and rolled off at 1400mA when about 2.5mW. Although the power was measured under pulsed injection, the saturation and roll-off was attributed to heating effects. "A significant improvement in optical output power is expected for the SLDs by applying anti-reflection coating to the cavity facets and adopting proper packaging with good heat dissipation," the team writes.

Current–voltage and capacitance–voltage measurements were used to assess the resistance–capacitance (RC) bandwidth of the devices. The series resistance was estimated at 2.8Ω for the SLD, on the basis of the linear section of the current–voltage plot between 150mA and 400mA injection. A similar estimate for the laser diode gave 2.6Ω series resistance. A 1MHz modulated signal with the diode biased between –8V and +2V gave a capacitance estimate of 32.5pF at –4V bias, representing deep depletion in the diode (34.4pF for the laser diode). The RC time constant for the SLD was 90ps, representing a frequency of 1.77GHz. This opens up VLC opportunities.

## Vertical light-emitting diodes

A different group of researchers in China have integrated high-power, reliable vertical InGaN light-emitting diodes on 4-inch silicon substrates using wafer bonding methods [Shengjun Zhou et al, Optics Express, vol27, pA1506, 2019]. The team from Wuhan University, Changchun Institute of Optics, Fine Mechanics and Physics, and Xiamen Changelight Co Ltd used a number of measures to improve the performance of the final LEDs by reducing current crowding and protecting the device structure from humidity.

The device layers were grown on patterned sapphire substrates using MOCVD (Figure 6). The LED fabrication began with inductively coupled plasma (ICP) etch into 1mmx1mm mesas for electrical isolation. A $SiO_2$ current-blocking layer (CBL) was applied using plasma-enhanced CVD and patterning into 15µm-wide strips via photolithography and buffered-oxide wet etch (Figure 7).

Ion-beam sputtering applied a 100nm silver film as reflector, followed by titanium/tungsten as a diffusion barrier. After electron-beam deposition of a platinum/titanium cap, rapid thermal annealing at 600ºC was used to improve the GaN/silver ohmic contact.

The 4"-diameter p-Si final device substrate was prepared by adding multi-layers of titanium/platinum/gold and a titanium/platinum cap. A 2.5µm layer of indium was applied to the p-Si substrate before thermal compression bonding at 230ºC. One feature of the titanium adhesion layer was that it also acted as a barrier against poisoning of the p-Si with gold. Platinum contamination of the p-Si was also avoided, according to energy-dispersive x-ray analysis.

A 248nm krypton-fluoride excimer laser was used to perform lift-off separation of the sapphire growth substrate.

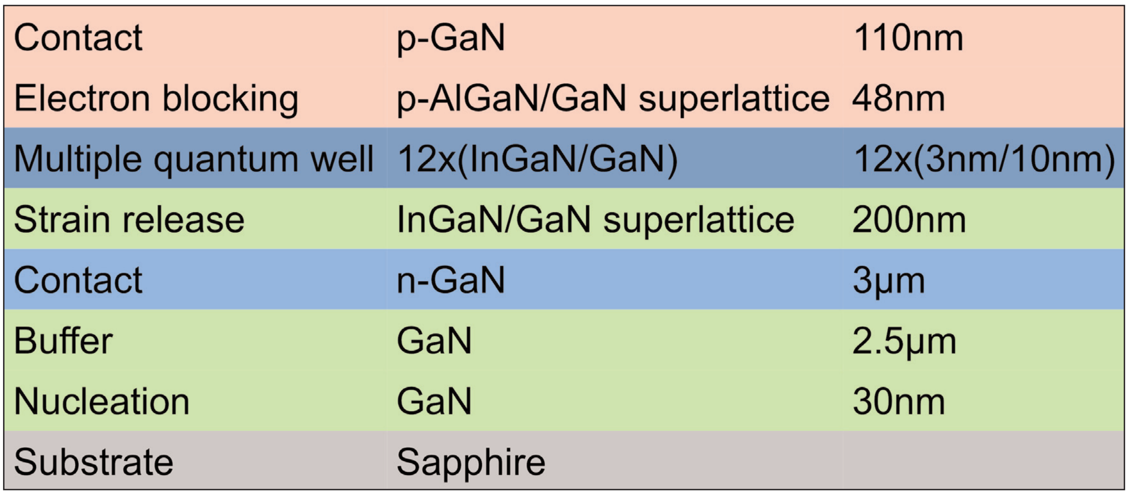

| | | |
|---|---|---|
| Contact | p-GaN | 110nm |
| Electron blocking | p-AlGaN/GaN superlattice | 48nm |
| Multiple quantum well | 12x(InGaN/GaN) | 12x(3nm/10nm) |
| Strain release | InGaN/GaN superlattice | 200nm |
| Contact | n-GaN | 3µm |
| Buffer | GaN | 2.5µm |
| Nucleation | GaN | 30nm |
| Substrate | Sapphire | |

**Figure 6. Vertical LED device layer MOCVD growth sequence.**

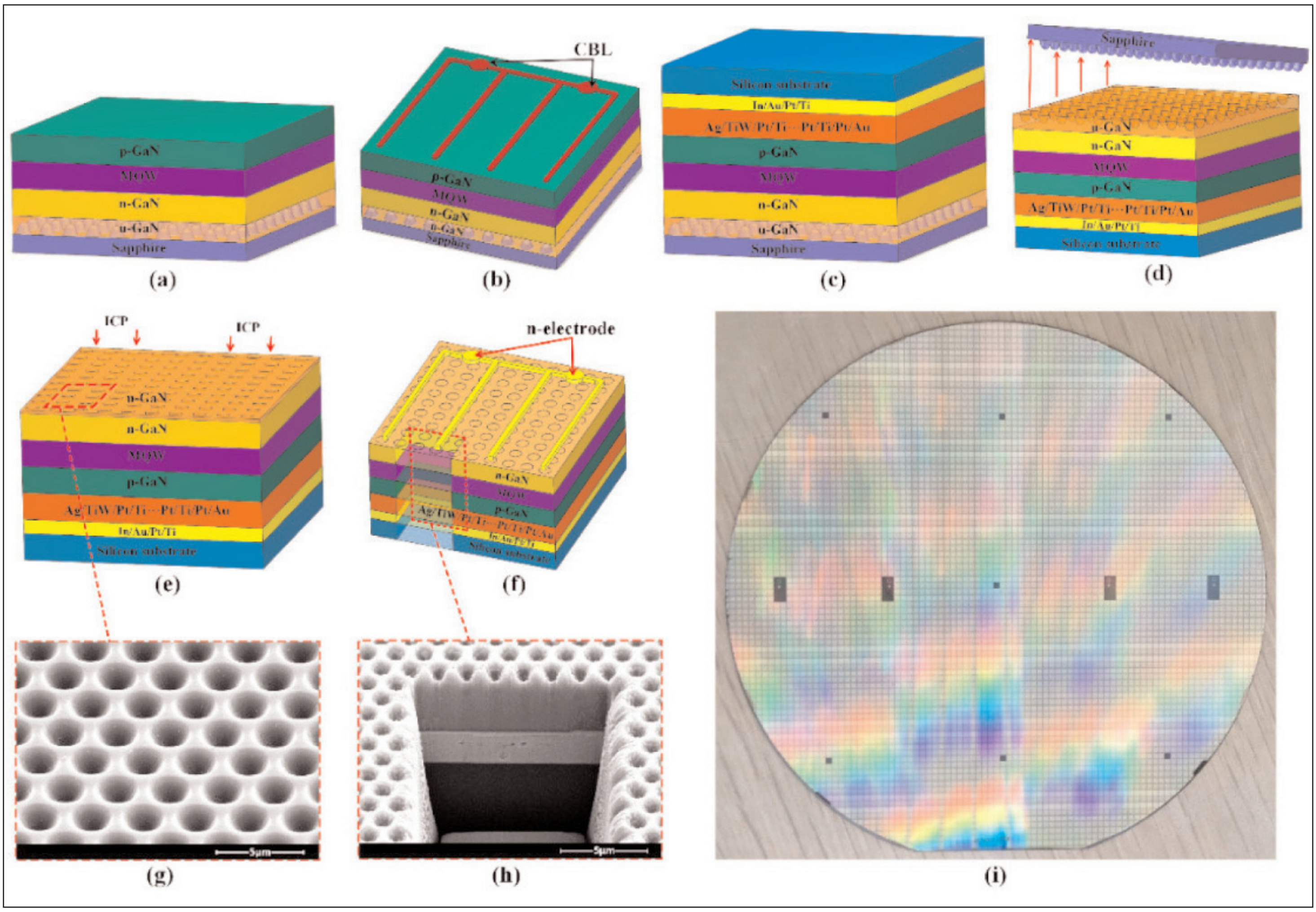

**Figure 7. Fabrication process of LEDs: (a) MOCVD growth; (b) defining $SiO_2$ CBL; (c) metal deposition and bonding to silicon wafer; (d) laser lift-off (LLO) removal of sapphire substrate; (e) ICP etch to n-GaN contact; (f) deposition of p- and n- electrodes. (g) Scanning electron microscope (SEM) image of exposed n-GaN surface with hemispherical dimples after LLO and ICP etching. (h) Cross-section SEM image of LEDs bonded to silicon wafer. (i) Photograph of LEDs on 4" silicon wafer; colors arise from thin-film interference effects.**

This was followed by ICP etch down to the n-GaN contact layer.

The n-GaN was treated with potassium hydroxide (KOH) or phosphoric acid ($H_3PO_4$) solution to texture the surface for improved light extraction. Chromium/platinum/gold was used to form the p- and n-electrodes for the LED. The n-contact metals were formed into 12μm-wide fingers.

The $SiO_2$ CBL around the opaque electrodes directed current away from this region and made for more uniform current density in the light-emitting areas, according to simulations. Along with the vertical structure, it was hoped the CBL would reduce self-heating, making for more efficient performance over lateral structure devices. Current crowding leading to self-heating is a major problem in conventional lateral structure LEDs.

The vertical LED structure enabled much lower forward voltages for a given current injection — 2.87V at 350mA, compared with 3.52V with a conventional lateral LED structure (Figure 8). Lower forward voltage indicates lower input power and hence higher power efficiency. The light output power (LOP) for a given current injection was also higher in the vertical LED: the lateral LED output saturated at ~320mA, while the vertical device increased in light power up to 1300mA. "The absence of premature LOP saturation in V-LEDs was attributed to reduced current crowding and enhanced heat dissipating compared to L-LEDs," the team writes.

With 350mA, the vertical LED output power was 501mW, beating a previous report of a GaN vertical blue LED of ~450mW at the same injection. The researchers comment: "The higher LOP demonstrated in this work confirmed that integrating the optimized metallization scheme, $SiO_2$ CBL and surface texturing by KOH wet etching is an effective approach to higher performance V-LEDs."

[I get a crude output/input power efficiency value of 50% (501mW/(2.87Vx350mA).]

The researchers also developed a platinum/titanium protective wrap-around layer for the silver/titanium-

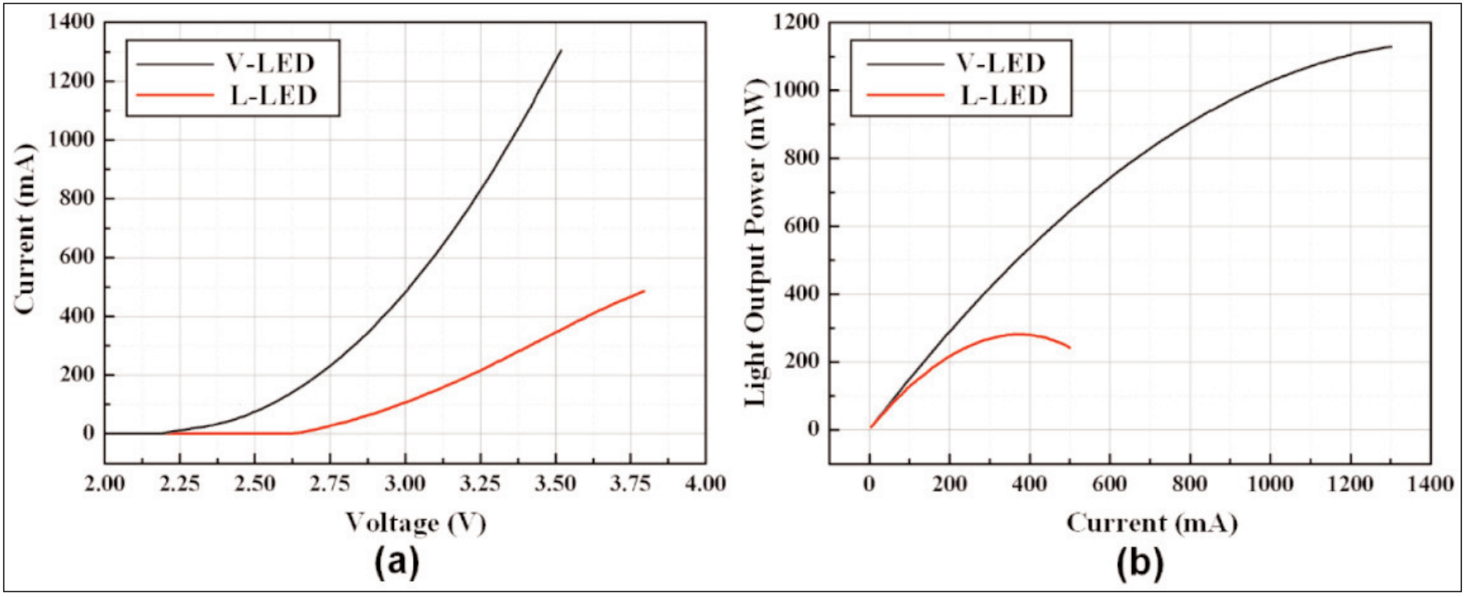

**Figure 8. (a) Current–voltage profiles of lateral (L-) and vertical (V-)LEDs. (b) Light output power–current characteristics.**

tungsten alloy structure. The wrap-around structure protected the mirror contact from humidity degradation. Operation at 85ºC and 85% relative humidity degraded the performance of LEDs without lateral wrap-around protection over 1000 hours. By contrast, the LEDs with wrap-around platinum/titanium showed "negligible optical degradation even after an aging time of 1008h," according to the researchers. ■

*The author Mike Cooke is a freelance technology journalist who has worked in the semiconductor and advanced technology sectors since 1997.*